



Magnetic nanoparticles detection of C-Reactive Protein combined with neutrophil to lymphocyte ratio to predict the occurrence of anastomotic fistula after rectal cancer surgery

Guolei Song^{1,2}, Han Guo³, Congqiao Jiang², Yi Shi², Mulin Liu^{1,2*}

¹First Clinical Medical College, Jinan University, Guangzhou, 510632, Guangdong Province, China

²Department of Gastrointestinal Surgery, The First Affiliated Hospital of Bengbu Medical College, Bengbu, 233004, Anhui Province, China

³The Fourth Ward of General Surgery, The First Affiliated Hospital of Bengbu Medical College, Bengbu, 233004, Anhui Province, China

ARTICLE INFO

Original paper

Article history:

Received: July 09, 2022

Accepted: August 21, 2022

Published: August 31, 2022

Keywords:

PAA-Au/Fe₃O₄, CRP combined with NLR, rectal cancer, anastomotic fistula

ABSTRACT

It aimed to explore the effect of C-reactive protein (CRP) combined with neutrophil to lymphocyte ratio (NLR) in the early prediction of anastomotic leakage (AL) after rectal cancer surgery and to improve the prediction accuracy. In this study, gold (Au)/ferroferric oxide (Fe₃O₄) magnetic nanoparticles were first synthesized and modified with polyacrylic acid (PAA). After modification, they underwent CRP antibody detection. Then, 120 patients with rectal cancer who underwent Dixon surgery were selected as the research objects to investigate the sensitivity and specificity of CRP combined with NLR in predicting AL. It was found that the diameter of the Au/Fe₃O₄ nanoparticles prepared in this study was about 45 nm. After adding 60 μg of antibody, the diameter of PAA-Au/Fe₃O₄ was 226.5 nm, the dispersion coefficient was 0.16, the standard curve between CRP concentration and luminous intensity was $y = 8,966.5x + 2,381.3$, and $R^2 = 0.9944$. Besides, the correlation coefficient was $R^2 = 0.991$, and the linear regression equation was $y = 1.103x - 0.0022$ compared with the nephelometric method. By analyzing the receiver operating characteristic (ROC) curve of CRP combined with NLR to predict AL after Dixon surgery, the cut-off point was 0.11 on the first day after the surgery, the area under the curve was 0.896, the sensitivity was 82.5%, and the specificity was 76.67%. The cut-off point on the third day after the surgery was 0.13, the area under the curve was 0.931, the sensitivity was 86.67%, and the specificity was 90%. On the fifth day after the surgery, the cut-off point, the area under the curve, the sensitivity, and the specificity were 0.16, 0.964, 92.5%, and 95.83% in turn. In conclusion, PAA-Au/Fe₃O₄ magnetic nanoparticles could be used for clinical examination of patients with rectal cancer, and CRP combined with NLR could improve the prediction accuracy of AL after rectal cancer surgery.

Doi: <http://dx.doi.org/10.14715/cmb/2022.68.8.21>

Copyright: © 2022 by the C.M.B. Association. All rights reserved.

Introduction

Rectal cancer is a common malignant tumor of the digestive tract. Studies have shown that there are no less than 1.2 million new rectal cancer patients worldwide, and the number of deaths due to rectal cancer is no less than 600,000. Besides, this data is increasing year by year (1). The incidence of rectal cancer ranks among the top three of all cancers, and its mortality rate ranks fourth. According to data released by the World Health Organization (WHO), the incidence and deaths of rectal cancer in China rank first in the world (2). The missed diagnosis rate of rectal cancer patients in China is relatively high, and the early diagnosis of patients is not higher than 40%, resulting in a large number of patients who have gone to the best diagnosis time. This is also one of the reasons for the high mortality of rectal cancer patients (3).

At present, the treatment of rectal cancer is still based on surgical treatment. Surgical resection is the most effective method for the treatment of rectal cancer. The surgical method depends on the preoperative staging and the middle left pole from the anal margin. Currently, commonly

used Dixon surgery can improve the anal preservation rate of patients to a large extent but inevitably increases the risk of postoperative AL (4). AL mostly occurs 5-7 days after Dixon. When one patient suffers from AL, it increases the patient's physical and mental pain and medical expenses, raises the local recurrence rate, and even requires a second surgery, which poses a great threat to the patient's life and health (5). Studies have shown that the occurrence of AL is usually accompanied by clinical symptoms such as fever, elevated white blood cells, and dyspnea. However, such symptoms have low specificity and are difficult to be used for early detection of postoperative AL of rectal cancer. Therefore, remedial measures are usually taken after the occurrence of AL in clinical practice (6). Since the inflammatory response is accompanied by the development of a variety of diseases, and the changes of inflammatory factors are usually earlier than the appearance of the clinical symptoms of the disease, the inflammatory response can be used as an indicator to predict the occurrence of a certain disease (7).

In recent years, scientific research has found that CRP has a certain value in predicting AL after rectal cancer sur-

* Corresponding author. Email: liumulin2022@yandex.com

gery. As a marker of the acute phase of infectious diseases, CRP can judge whether the body is infected or not in the early stage of infection of a certain disease, and is not affected by individual differences and therapeutic drugs. However, due to the time delay between the examination and the result, CRP blood examination only plays a small part in the early diagnosis of the disease, and the CRP detection time is long, which could not affect the management decision (8). NLR test is simpler than the CRP test, which can reflect the degree of inflammation and can be used to predict the prognosis of patients with malignant tumors, but it is rarely applied in the early prediction of the occurrence of AL (9, 10). Based on the above reasons, a magnetic nanomaterial was designed and synthesized in this study, making it have a more efficient and specific adsorption capacity for CRP so as to improve the detection efficiency. What's more, CRP and NLR were as indicators of inflammatory response observations, thereby evaluating the predictive value of CRP combined with NLR for AL after rectal cancer surgery.

Materials and Methods

Research objects

In this study, 120 patients who were diagnosed with rectal cancer pathologically after surgery in the Department of Gastroenterology and Gastroenterology of The First Affiliated Hospital of Bengbu Medical College from December 2019 to December 2020 were selected as the research objects, and all patients were treated with surgical resection in this hospital. Among them, 72 were male patients and 48 were female patients, aged 19-78 years, with an average age of 56 years old. Senior doctors of the original source operated on all patients. The ethics committee approved this study of The First Affiliated Hospital of Bengbu Medical College. All patients and their family members understood this case, and an informed consent form for the surgery was signed.

The criteria for inclusion were defined to include patients who were older than 18 years old, and the gender was not limited; were determined to be rectal cancer by histopathology; had the Dixon surgery; had complete clinical data and had certain communication ability; did not suffer from other serious infectious diseases or malnutrition.

The criteria for exclusion were defined to include patients who were younger than 18 years old, received radiotherapy or chemotherapy for rectal cancer before admission, had emergency surgery, suffered from clinical infection before the surgery, were checked before admission, finding that rectal cancer developed distant metastasis, and had incomplete clinical data or lack of communication skills.

Preparation of Au/Fe₃O₄ magnetic nanoparticles

In this study, Au nanoparticles were used as seeds and Fe(CO)₅ was thermally decomposed at high temperature to prepare Au/Fe₃O₄ magnetic nanoparticles. This preparation was completed in two steps. First, the oil-phase gold nanoparticles were prepared by the oleylamine reduction method. 30 mL of 1-octadecene was weighed and put into a 500 mL four-neck flask. Then, 4 mL of oleylamine was added, and the magnetic stirring was turned on. The speed was controlled to about 1,400 r/min for stirring, so the

temperature was heated up to 75 °C. While heating, 1.0 g of HAuCl₄ was weighed and added with 40 mL of 1-octadecene and 4 mL of oleylamine mixture for ultrasonic dissolution. After the system was heated to 75 °C, the pre-prepared HAuCl₄ solution was added, and the stirring was under 75 ± 2 °C for 6 hours. After the reaction was over, the temperature was naturally cooled to room temperature, and it was filtered with suction after settling with isopropanol for 40 minutes. After suction filtration, the filter cake was washed with an appropriate amount of isopropanol. After repeated washing and suction filtration three times, the filter cake was re-dispersed in 180 mL of n-hexane and stored at 4 °C.

After the preparation technology of oil phase gold nanoparticles, 40 mL of 1-octadecene, 40 mL of gold seeds, 2 mL of oleylamine, and 2 mL of oleic acid were added into a 500mL four-necked flask in turn. The speed was controlled to 1,400 r/min and there was magnetic stirring for 30 minutes so as to slowly heat up to 150 °C. After the temperature reached 150 °C, 0.4mL Fe(CO)₅ was quickly added into the flask, which was stirred and heated to 290 °C for 1 hour. After the reaction, the nitrogen was removed, the air was introduced for 1 hour, and it was placed on a permanent magnet for magnetic separation. After the magnetic separation was clean, the supernatant was discarded, and the washing was repeated three times with absolute ethanol, and the Buchner funnel was applied to drain. The filter cake was re-dispersed in 40 mL of n-hexane and ultrasonic for 2-3 minutes, the solid content in the solution was determined, and it was stored at 4 °C for later use.

Characterization of Au/Fe₃O₄ magnetic nanoparticles

The morphology of Au/Fe₃O₄ magnetic nanoparticles was characterized by transmission electron microscope (TEM), and the crystallographic properties of Au/Fe₃O₄ magnetic nanoparticles were analyzed by X-ray diffraction (XRD). The thermal stability of Au/Fe₃O₄ magnetic nanoparticles was analyzed by thermogravimetric analysis (TGA), and Nicomp380/ZLS nanoparticle size analyzer was employed to analyze the polydispersity index (PDI) of Au/Fe₃O₄ magnetic nanoparticles.

Coating of CRP antibody

After Au/Fe₃O₄ magnetic nanoparticles were modified with monodisperse PAA, 150 μL (5mg/L) were weighed and transferred into a 2 mL centrifuge tube, and 0.5 mL phosphate buffer saline (PBS) buffer was added into the tube, so that it was shaken well and placed on a magnetic grate for separation. Then, the supernatant was discarded, and 80 μL of 1-(3-Dimethylaminopropyl)-3-ethylcarbodiimide hydrochloride (EDC) solution (10 mg/L) was added, and the mixed solution in the tube was shaken well, which was ultrasonically reacted for 1 hour. After the reaction was over, it was placed on a magnetic grate for separation, the supernatant was discarded, and 150 μL of PBS was added to mix well. A certain concentration of CRP was added to the activated PAA-Au/Fe₃O₄ magnetic nanoparticles, which were mixed well and placed in a constant temperature shaking incubator. Besides, the temperature was controlled at 36 °C and reacted for 1 hour. After the reaction was completed, the magnetic grate was separated, the supernatant was discarded, and an appropriate amount of PBS buffer was adopted to wash. After washing, 0.8

mL of the blocking agent was added and the mixture was mixed well, which was put in a constant temperature shaking incubator. What's more, the temperature was controlled at 36 °C, and there was a reaction for 2 hours. After the reaction was over, 450 μ L of PBS buffer was employed to wash, and the mixture was added with 0.8 mL of preservation solution, mixed well, and set aside.

AL diagnostic criteria

A patient could be diagnosed as AL when one or more of the following symptoms appeared after the surgery. First, the patient suddenly developed symptoms such as persistent fever, abdominal pain, and peritonitis after the surgery. Second, the patient's drainage tube drainage fluid suddenly increased, and the drainage fluid was cloudy and smelly with feces. Third, an abscess around the anastomotic stoma was found after an imaging examination. Fourth, contrast agent leakage was found in the contrast agent examination, and the anastomotic stoma was broken in some patients during the rectal examination.

Observation indicators

The preoperative CRP and NLR of the patient were calculated for the fasting peripheral blood drawn within 24 hours after admission, and the postoperative CRP and NLR were calculated for the early morning fasting blood sampling on the 1st day after the surgery, the 3rd day after the surgery, and the 5th day after the surgery. The ROC of patients should be calculated based on the calculated results.

Statistical analysis

SPSS23.0 software was used for the statistical processing of the data of this study. First, whether the measurement data met the normal distribution should be determined. If it met the normal distribution, the t-test was adopted. If it did not meet the normal distribution, the independent sample Mann-Whitney U test was employed. The measurement data were tested by using the calculation results to draw the ROC curve and calculate the area under the curve to evaluate the significance and accuracy of CRP and NLR in predicting AL on the 1st day, the 3rd day, and the 5th day after surgery. In addition, $P < 0.05$ indicated that the difference was statistically substantial.

Results

Characterization of Au/Fe₃O₄ magnetic nanoparticles

In this study, TEM was applied to characterize the morphology of the prepared Au/Fe₃O₄ magnetic nanoparticles. It was found that the prepared Au/Fe₃O₄ magnetic nanoparticles had regular and uniform shapes, regular crystal phases, and a particle size of about 45 nm. Furthermore, the morphology of the prepared Au/Fe₃O₄ magnetic nanoparticles under TEM is shown in Figure 1a.

XRD was employed to analyze the structure of the Au/Fe₃O₄ magnetic nanoparticles prepared in this study so as to draw the XRD pattern of the Au/Fe₃O₄ magnetic nanoparticles, and the results were presented in Figure 2. It indicated that the sample had the highest diffraction peak intensity at 18.45 °, and the XRD standard card corresponded to gold nanoparticles (JCPDS card No. 04-0784). In addition, the diffraction peaks of different intensities also appeared at diffraction angles of 14.16 °, 16.43 °,

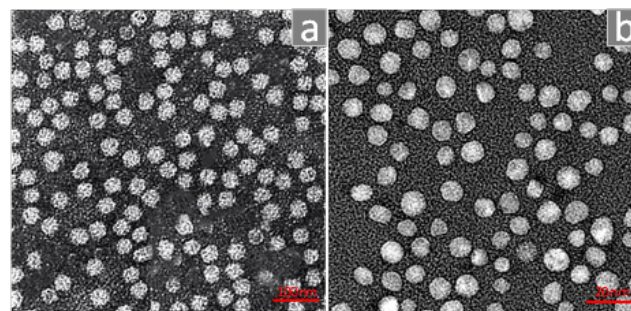


Figure 1. TEM images. (Note: a: TEM image of Au/Fe₃O₄ magnetic nanoparticles; b: TEM image of gold nanoparticles.)

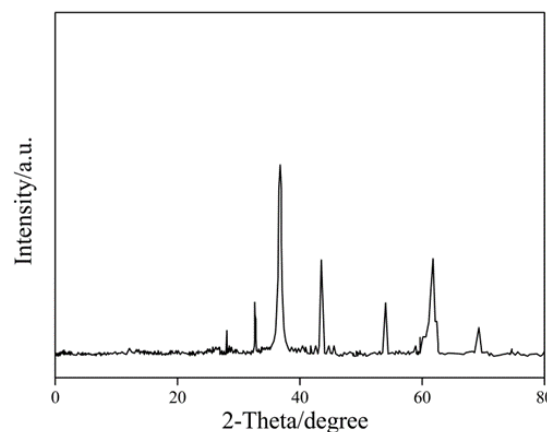


Figure 2. XRD diffraction pattern of Au/Fe₃O₄ magnetic nanoparticles.

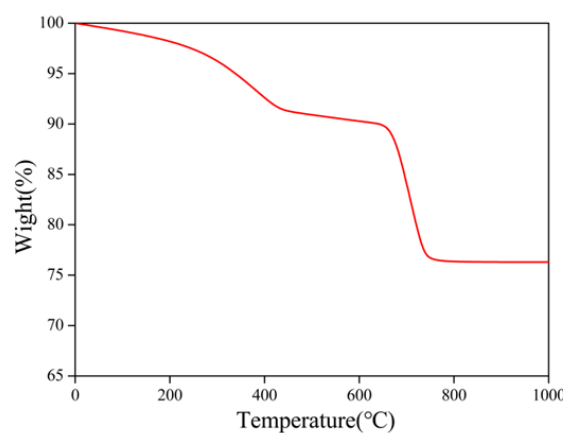


Figure 3. Thermogravimetric analysis curve of Au/Fe₃O₄ magnetic nanoparticles.

21.61 °, 27.34 °, 30.66 °, and 34.44 °. The XRD standard card correspondingly found the phase of gold nanoparticles at diffraction angles of 14.16 ° and 16.43 ° (JCPDS card No. 04-0784). Moreover, 21.61°, 27.34°, 30.66°, and 34.44° diffraction angles were the phase of Fe₃O₄ nanoparticles (JCPDS card No.79-0418). According to the corresponding analysis of different crystal planes, it was found that the Fe₃O₄ in the Au/Fe₃O₄ magnetic nanoparticles prepared in this study was a typical cubic reverse spinel structure.

TGA was performed on the Au/Fe₃O₄ magnetic nanoparticles prepared in this study, the surface organic molecules of the Au/Fe₃O₄ magnetic nanoparticles were analyzed, and the corresponding thermogravimetric curve was drawn, which was displayed in Figure 3. The thermogravimetric curve showed that there were 2 weight loss

processes after the temperature was higher than 300 °C. When the temperature was lower than 160 °C, the curve had a small amount of mass loss. It was speculated that the reason might be the adsorption of Au/Fe₃O₄ magnetic nanoparticles on the surface. Due to the volatilization of organic solvents, a rapid weight loss process occurred at 300-450 °C, about 6.3% weight loss. Thus, it was speculated that the cause of this mass loss was due to the analysis of the outermost layer of oleic acid. In addition, the second occurred at 650-750 °C, and there was about 13.5% weight loss, which was presumed to be due to the loss of more tightly bound oleic acid. Thermogravimetric analysis revealed that the surface of Au/Fe₃O₄ magnetic nanoparticles was coated with oleic acid, and the total weight loss during the whole thermogravimetric analysis was about 23.1%. That was, the coating amount of oleic acid on the surface of Au/Fe₃O₄ magnetic nanoparticles accounted for about 23.1 % of the entire nanoparticle.

CRP detection by PAA-Au/Fe₃O₄ magnetic nanoparticles

The dispersion performance of the PAA-Au/Fe₃O₄ magnetic nanoparticles coated with CRP antibody was a key factor in the immunoassay process. The agglomeration of the PAA-Au/Fe₃O₄ magnetic nanoparticles would affect the sensitivity and detection range of the immunoassay. In this study, the Nicomp380/ZLS nanoparticle size analyzer was used to characterize the particle size and dispersibility of the PAA-Au/Fe₃O₄ magnetic nanoparticles prepared this time. Above all, PAA-Au/Fe₃O₄ magnetic nanoparticle size under the additional amount of 8 kinds of antibodies was respectively detected in this study, and the test results are shown in Figure 4. From the previous results, the diameter of the Au/Fe₃O₄ magnetic nanoparticles prepared in this study was about 45 nm. After the PAA modification, the average particle size increased markedly. However, the growth of particle size was not proportional to the increase of antibodies, with the increase in antibody amount indicating that there was no specific relationship between the two.

Figure 4 disclosed that the particle size of PAA-Au/Fe₃O₄ magnetic nanoparticles was 226.5 nm when the amount of antibody was 60 µg. When the amount of antibody was greater than 60 µg, the particle size of the nanoparticles elevated hugely, so 60 µg was chosen. The amount of antibody was analyzed for the dispersion of PAA-Au/Fe₃O₄ magnetic nanoparticles. Three parallel tests were performed during the detection and analysis, and the average value of each indicator was taken. The analysis results were shown in Table 1, suggesting that the average particle size of PAA-Au/Fe₃O₄ magnetic nanoparticles was 226.5 nm and the average PDI was 0.16 when the amount of antibody added was 60 µg. It was found that the PDI remained at a low level after the addition of the antibody, indicating that the agglomeration that occurred during the modification of the antibody molecule was not

obvious.

CRP standards with different concentration gradients were selected, and the corresponding luminous intensity was calculated, so as to draw the standard curve with the concentration as the abscissa and the luminous intensity as the ordinate. The results were shown in Figure 5a, revealing that the luminous intensity was directly proportional to the CRP concentration, and the linear relationship was good. Besides, the standard curve was $y = 8,966.5 x + 2,381.3$, and $R^2 = 0.9944$.

After the standard curve was drawn, Dixon preoperative clinical serum samples of 30 patients were selected randomly and diluted with 1 × PBS. Then, the samples were measured. What's more, the current clinical scatter turbidimetric method was introduced for comparison. A correlation diagram was drawn according to different detection methods, and the results are displayed in Figure 5b. The results meant that the correlation coefficient of

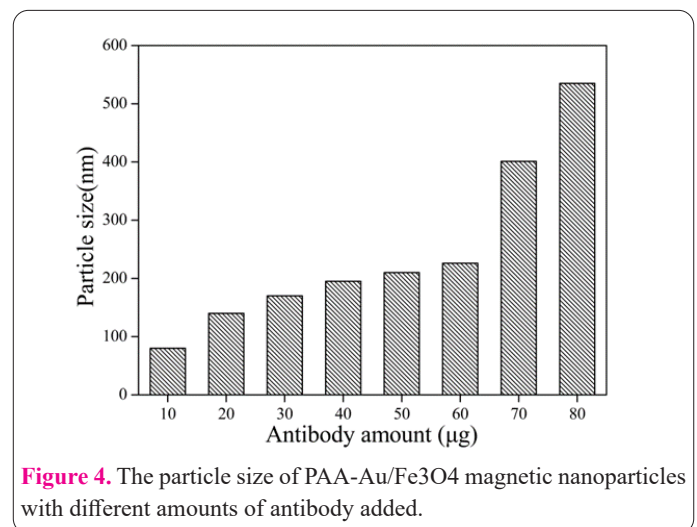


Figure 4. The particle size of PAA-Au/Fe₃O₄ magnetic nanoparticles with different amounts of antibody added.

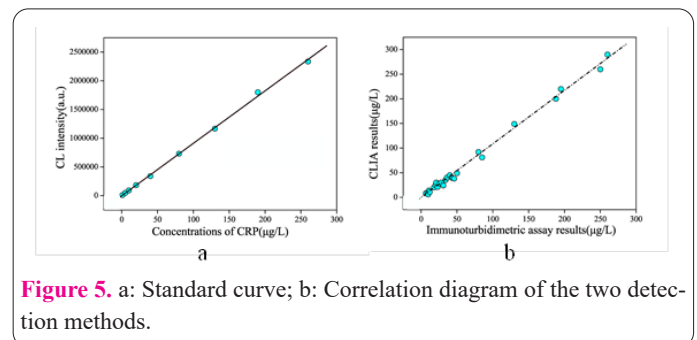


Figure 5. a: Standard curve; b: Correlation diagram of the two detection methods.

Table 1. Particle size and dispersion of PAA-Au/Fe₃O₄ magnetic nanoparticles with antibody amount of 60 µg.

	PDI	Particle size (nm)
1	0.14	194.3
2	0.18	246.7
3	0.16	238.5
Average value	0.16	226.5

Table 2. Comparison of average CRP between normal patients and AL patients after surgery.

Time	Anastomotic normal patients	Patients with AL	P
Before surgery	62.42	64.11	/
On the 1 st day after surgery	71.05	90.38	0.033
On the 3 rd day after surgery	82.35	135.44	0.012
On the 5 th day after surgery	64.49	164.31	0.006

the two detection methods was $R^2 = 0.991$, and the linear regression equation was $y = 1.103x - 0.0022$. The correlation between the two detection methods was good, which indicated that the PAA-Au/Fe₃O₄ magnetic nanoparticles prepared in this study were adopted to measure CRP. Thus, it could be used for the clinical examination of patients with rectal cancer.

Postoperative AL in patients with rectal cancer predicted by CRP combined with NLR

After Dixon surgery in 120 patients, 14 cases developed AL, with an AL incidence rate of 11.67%. All AL patients recovered after receiving conservative treatment or intestinal stoma, and no patients died. The results of this study found that the CRP indicators of patients who did not develop AL after the surgery increased on the first day and then gradually decreased to normal. The CRP of AL patients rose obviously on the first day after surgery and continued to grow over time. Table 2 indicated that the difference in CRP between patients with normal anastomosis and AL patients was statistically substantial ($P < 0.05$).

The best cut-off point of the CRP change value of 120 patients was calculated based on the ROC curves. According to the ROC curves of the patients (Figure 6), the cut-off point was 73.33 on the first postoperative day, the area under the curve was 0.801, the sensitivity was 80.83%, and the specificity was 59.98%. The cut-off point on the third day after the surgery was 138.35, the area under the curve was 0.936, the sensitivity was 85.83%, and the specificity was 82.5%. What's more, the cut-off point, the area under the curve, the sensitivity, and the specificity on the fifth day after the surgery were 85.41, 0.968, 89.17%, and 81.67% in turn.

The NLR of 120 patients was tested, and the results showed that the NLR of patients who did not develop AL after the surgery increased on the first day and then gradually reduced to normal over time. The NLR of AL patients elevated greatly on the first day after surgery. There was still a tendency to increase on the third day and decrease to a certain extent on the fifth day (Table 3). There was a statistical difference in postoperative NLR between patients with normal anastomosis and AL patients ($P < 0.05$).

Similarly, the best cut-off point of the change in NLR of 120 patients was calculated based on the ROC curves (Figure 7). Moreover, the cut-off point of patients on the first day after the surgery was 4.9, the area under the curve was 0.692, the sensitivity was 61.67%, and the specificity was 45.39%. On the third day after surgery, the cutoff point was 12.2, the area under the curve was 0.789, the sensitivity was 72.5%, and the specificity was 66.67%. In addition, the cut-off point on the 5th postoperative day was 9.3, the area under the curve was 0.801, the sensitivity was 65.83%, and the specificity was 78.33%.

In order to further improve the accuracy of predicting postoperative AL in patients with rectal cancer, NLR

monitoring was combined with CRP monitoring, and the combined factor was recalculated to draw the corresponding ROC curves, which are shown in Figure 8. According to the ROC curves, the best cut-off point for the change of CRP and NLR in 120 patients was calculated. What's more, the cut-off point was 0.11 on the first day after the surgery, the area under the curve was 0.896, the sensitivity was 82.5%, and the specificity was 76.67%. The cut-off point, the area under the curve, the sensitivity, and the specificity on the third day after surgery were 0.13, 0.931, 86.67%, and 90%, respectively. On the postoperative fifth day, the cut-off point, the area under the curve, the sensitivity, and the specificity were 0.16, 0.964, 92.5%, and 95.83% in sequence.

Discussion

Rectal cancer is one of the most common causes of malignance-related death worldwide. With the continuous

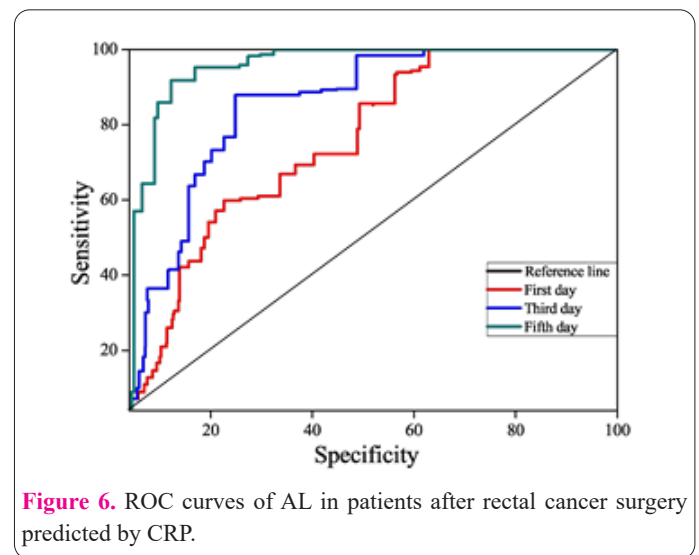


Figure 6. ROC curves of AL in patients after rectal cancer surgery predicted by CRP.

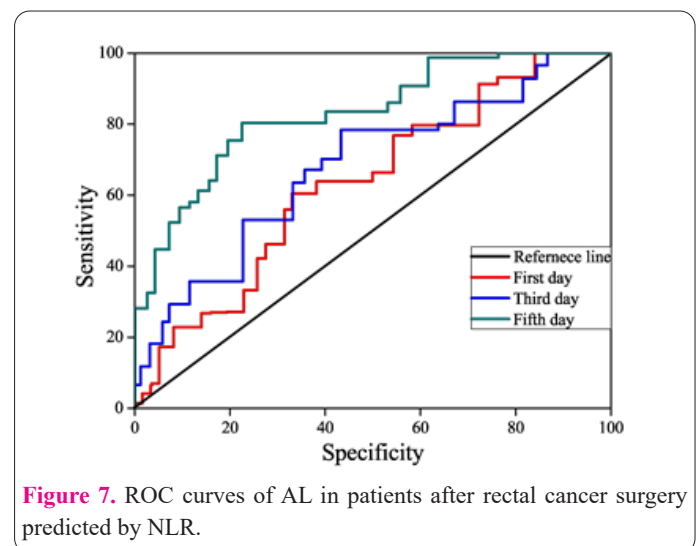


Figure 7. ROC curves of AL in patients after rectal cancer surgery predicted by NLR.

Table 3. Comparison of average NLR between normal patients and AL patients after surgery.

Time	Anastomotic normal patients	Patients with AL	P
Before surgery	4.41	4.65	/
On the 1 st day after surgery	12.88	16.22	0.046
On the 3 rd day after surgery	8.62	18.35	0.001
On the 5 th day after surgery	5.19	14.19	0.001

change in people's living habits and diet level, the incidence of rectal cancer has an increasing trend year by year, and its particularity makes patients often miss diagnosis (11). At present, surgical resection is still the main treatment for rectal cancer, but postoperative AL is the most common serious complication (12). According to reports, the incidence of AL after Dixon surgery is about 3-19% per month. Once the patient develops AL, it will not only increase the patient's medical expenses and physical pain but may also promote tumor recurrence, metastasis, and patient prognosis, and even life-threatening in severe cases (13). Therefore, how to detect and treat AL early and take preventive measures early is the key to reducing the incidence of AL.

With the deepening of research on the relationship between tumors and inflammation, people realize that the disease progression of tumor patients depends not only on the characteristics of the tumor, but also on the inflammatory response of the host. Studies have confirmed that inflammatory mediators have a role in the transduction factors of rectal cancer. Certainly, CRP and NLR are related to the prognosis of a variety of tumors, and high levels of CRP and NLR usually indicate poor prognosis (14). The detection of CRP is not affected by individual differences and therapeutic drugs, but there is a time delay between the examination and the results, and the diagnostic sensitivity is poor, which can't affect management decisions. NLR detection is simple and is often used to predict the postoperative prognosis of patients with malignant tumors (15-18), but there are few studies on the prediction of AL after colon cancer surgery.

In this study, Fe(CO)₅ was used as raw material to prepare Au/Fe₃O₄ magnetic nanoparticles with uniform particle size, and they were characterized by TEM, XRD, and TGA. The results found that the Au/Fe₃O₄ magnetic nanoparticles prepared in this study had a regular and uniform morphology, with a particle size of about 45 nm. XRD data showed that the Fe₃O₄ in the Au/Fe₃O₄ magnetic nanoparticles had a typical cubic reverse spinel structure. TGA analysis found that Au/Fe₃O₄ magnetic nanoparticles had oleic acid molecules attached to the surface, and their mass accounted for about 23.1% of the entire magnetic nanoparticles. Subsequently, the Au/Fe₃O₄ magnetic nanoparticles were modified with PAA and attached to the CRP antibody to detect the particle size and dispersion properties of the antibody-coated PAA-Au/Fe₃O₄ magnetic nanoparticles. It was found that the particle size increased with the amount of antibody added, but there was no specificity between the two. When the amount of antibody added was 60 µg, the average particle size reached 226.5 nm and the average PDI reached 0.16, which suggested that the nanoparticles did not agglomerate markedly when 60 µg antibody was added. Finally, a standard curve of CRP concentration and luminescence intensity was drawn, and 30 clinical serum samples of rectal cancer patients were randomly selected based on the standard curve for detection, and compared with the nephelometric method. The results revealed that the two detection methods were highly correlated, so the PAA-Au/Fe₃O₄ magnetic nanoparticles could be used for clinical examination of patients with rectal cancer.

CRP and NLR were investigated and analyzed in turn to predict AL after Dixon surgery. Then, CRP and NLR were combined in order to improve the accuracy of pre-

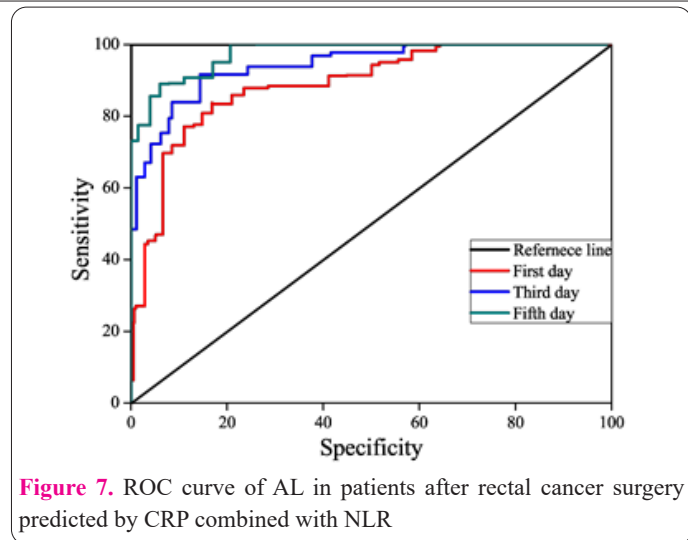


Figure 7. ROC curve of AL in patients after rectal cancer surgery predicted by CRP combined with NLR

dicting AL after Dixon surgery. The results indicated that the sensitivity was 82.5% and the specificity was 76.67% on the first postoperative day; the sensitivity was 86.67% and the specificity was 90% on the third postoperative day; the sensitivity was 92.5% and the specificity was 95.83% on the fifth postoperative day. The above results suggested that CRP combined with NLR could effectively improve the accuracy of AL after Dixon surgery.

In this study, Au/Fe₃O₄ magnetic nanoparticles were successfully synthesized by the high-temperature thermal decomposition method. The particle size was about 45 nm, and the surface oleic acid accounted for about 23.1%. After 60 µg of CRP antibody was coated, the particle size was 226.5 nm, and the dispersion was good. This detection method was highly correlated with the turbidimetric method and could be used for the clinical examination of patients with rectal cancer. Through CRP combined with NLR to predict postoperative AL, it was found that this method could more accurately predict the occurrence of postoperative AL and had certain guiding significance for the clinical prediction of AL.

Fundings

The research is supported by: Natural science research project funding in Anhui Universities (No. KJ2017A219); Bengbu Medical College Research and innovation team Fund Project (No. BYKC201909).

References

1. Wilkinson N. Management of rectal cancer. *Surg Clin North Am* 2020; 100(3): 615-628.
2. Gu J. Problems and countermeasures of standardized surgical treatment for colorectal cancer. *Chin J Dig Surg* 2015; 14(6): 441-444.
3. Le KF, Zhao LH, Hong HP, Xu HZ, Li CG. Comparison of clinical effect between laparoscopic surgery and open surgery for treatment of early colorectal cancer. *Anhui Med J* 2015; (3): 337-339.
4. Gu J, Gao Q. Postoperative complications after rectal cancer surgery and management. *Zhonghua Wei Chang Wai Ke Za Zhi* 2017; 20(7): 740-743.
5. Shalaby M, Thabet W, Rulli F, Palmieri F, Saraceno F, Capuano I, Buonomo O, Giarratano G, Petrella G, Morshed M, Farid M, Sileri P. Anastomotic leakage following laparoscopic resection of low and mid rectal cancer. *Ann Ital Chir* 2019; 90: 57-67.
6. Kverneng Hultberg D, Svensson J, Jutesten H, Rutegård J, Matthiessen P, Lydrup ML, Rutegård M. The impact of anastomotic

- leakage on long-term function after anterior resection for rectal cancer. *Dis Colon Rectum* 2020; 63(5): 619-628.
7. Taylor CC, Millien VO, Hou JK, Massarweh NN. Association between inflammatory bowel disease and colorectal cancer stage of disease and survival. *J Surg Res* 2020; 247: 77-85.
 8. Kim WR, Han YD, Min BS. C-reactive protein level predicts survival outcomes in rectal cancer patients undergoing total mesorectal excision after preoperative chemoradiation therapy. *Ann Surg Oncol* 2018; 25(13): 3898-3905.
 9. Braun LH, Baumann D, Zwirner K, Eipper E, Hauth F, Peter A, Zips D, Gani C. Neutrophil-to-lymphocyte ratio in rectal cancer—novel biomarker of tumor immunogenicity during radiotherapy or confounding variable? *Int J Mol Sci* 2019; 20(10): 2448.
 10. Rashtak S, Ruan X, Druliner BR, Liu H, Therneau T, Mouchli M, Boardman LA. Peripheral neutrophil to lymphocyte ratio improves prognostication in colon cancer. *Clin Colorectal Cancer* 2017; 16(2): 115-123.e3.
 11. Oronsky B, Reid T, Larson C, Knox SJ. Locally advanced rectal cancer: The past, present, and future. *Semin Oncol* 2020; 47(1): 85-92.
 12. Hoshino N, Hida K, Sakai Y, Osada S, Idani H, Sato T, Takii Y, Bando H, Shiomi A, Saito N. Nomogram for predicting anastomotic leakage after low anterior resection for rectal cancer. *Int J Colorectal Dis* 2018; 33(4): 411-418.
 13. Kulikov EP, Kaminsky YD, Klevtsova SV, Nosov SA, Kholchev MY, Aristarkhov VG, Mertsalov SA. Profilaktika nesostoiatel'nosti shvov kolorektal'nogo anastomoza u bol'nykh rakom priamoĭ kishki [Prevention of Colorectal Anastomotic Leakage in Patients with Rectal Cancer]. *Khirurgiia (Mosk)* 2019; (11): 64-68.
 14. Keller DS, Windsor A, Cohen R, Chand M. Colorectal cancer in inflammatory bowel disease: Review of the Evidence. *Tech Colo-proctol* 2019; 23(1): 3-13.
 15. Alavi, M., Hamblin, M., Mozafari, M., Rose Alencar de Menezes, I., Douglas Melo Coutinho, H. Surface modification of SiO₂ nanoparticles for bacterial decontaminations of blood products. *Cell Mol Biomed Rep* 2022; 2(2): 87-97. doi: 10.55705/cmbr.2022.338888.1039.
 16. Alavi, M., Rai, M., Martinez, F., Kahrizi, D., Khan, H., Rose Alencar de Menezes, I., Douglas Melo Coutinho, H., Costa, J. The efficiency of metal, metal oxide, and metalloidal nanoparticles against cancer cells and bacterial pathogens: different mechanisms of action. *Cell Mol Biomed Rep* 2022; 2(1): 10-21. doi: 10.55705/cmbr.2022.147090.1023.
 17. Alavi, M., Rai, M. Antisense RNA, the modified CRISPR-Cas9, and metal/metal oxide nanoparticles to inactivate pathogenic bacteria. *Cell Mol Biomed Rep* 2021; 1(2): 52-59. doi: 10.55705/cmbr.2021.142436.1014
 15. Cikot M, Kasapoglu P, Isiksacan N, Binboga S, Kones O, Gemici E, Kartal B, Alis H. The importance of presepsin value in detection of gastrointestinal anastomotic leak: a pilot study. *J Surg Res* 2018; 228: 100-106.